Observational Study

Medicine®

OPEN

Accelerated diffusion-weighted imaging for lymph node assessment in the pelvis applying simultaneous multislice acquisition

A healthy volunteer study

Alexander Ciritsis, PhD*, Cristina Rossi, PhD, Magda Marcon, MD, Valerie Doan Phi Van, MD, Andreas Boss, MD, PhD

Abstract

To evaluate the feasibility of accelerated simultaneous multislice diffusion weighted sequences (SMS-DWI) for lymph node detection in the abdominopelvic region. Sequences were evaluated regarding the number and depiction of lymph nodes detected with SMS-DWI compared with conventional diffusion weighted sequences, the most suitable SMS- acceleration factor, signal-to-noise ratio (SNR), and the overall acquisition time (TA).

Eight healthy volunteers (4 men, 4 women; age range 21–39 years; median age 25 years) were examined in the pelvic region at 3T using a conventional DWI sequence and a SMS DWI sequence with different acceleration factors (AF: 2–3). Moreover, a SMS DWI sequence with AF 3 and higher slice resolution was applied. For morphological correlation of the lymph nodes and as a reference standard, an isotropic 3-dimensional T2-weighted fast-spin-echo sequence with high sampling efficiency (SPACE) was acquired. Two radiologists reviewed each DWI sequence and assessed the number of lymph nodes and the overall image quality. For each DWI sequence, SNR, SNR efficiency per time, contrast to noise (CNR), and ADC values were calculated. Values were statistically compared using a Wilcoxon test ($P < .05$).

Overall, scan time of SMS-DWI with AF2 (AF3) decreased by 46.9% (57.2%) with respect to the conventional DWI. Compared with the SPACE sequence, the detection rate was 89.6% for conventional DWI, 69.4% for SMS-DWI with AF2, and 59.9% for SMS-DWI with AF3. The highly resolved SMS-DWI with AF3 leads to a scan time reduction of 46.9% and detection rate of 83.0%. SNR and CNR were lower in the accelerated sequences (up to 51.0%, $P < .001$) as compared with the conventional DWI. SNR efficiency decreased to 19.3% for AF2 and to 31.3% for AF3. In the highly resolved dataset, an SNR efficiency reduction of 51.2% was found.

This study showed that lymph node detection in the abdominopelvic region with accelerated SMS-DWI sequences is feasible whereby an AF of 2 represents the best compromise between image quality, SNR, CNR, TA, and detection rate.

Abbreviations: ADC = apparent diffusion coefficient, AF = acceleration factor, CAIPIRIHIA = Controlled Aliasing in Parallel Imaging Results in Higher Acceleration, CNR = contrast to noise ratio, DWI = diffusion-weighted imaging, ICC = intra-class correlation, IVIM = intravoxel incoherent motion, MRI = magnetic resonance imaging, ROI = region of interest, SMS = simultaneous multislice, SMS-DWI = simultaneous multislice diffusion weighted sequences, SNR = signal to noise ratio, SPACE = sampling perfection with application optimized contrasts using different flip angle evolution, ss-EPI = single-shot spin echo echo-planar imaging, TA = acquisition time, TE = echo time, TR = repetition time.

Keywords: diffusion-weighted imaging, lymph node assessment, magnetic resonance imaging, multiband, simultaneous multislice

1. Introduction

Diffusion-weighted imaging (DWI) is a functional magnetic resonance imaging (MRI) technique, which has become an integral part in many clinical applications.[1,2] Mainly applied in brain-related applications in its early phase, DWI has become in recent years an important tool in the depiction and assessment of the abdominopelvic region.[3–6] By obtaining the image contrast from the differences in mobility of water protons, DWI provides information representing cellularity and the integrity of cellular membranes.[7] In particular, for the abdomen the evaluation of various diseases such as focal lesion detection can be facilitated by implementing diffusion-weighted sequences to the MR imaging protocol.[8,9] Beyond that, several studies have shown that DWI is also a reliable imaging procedure for the assessment of lymph nodes in the pelvic region.[10–12]

Usually, DWI sequences in the abdomen and pelvis are acquired in free breathing and rely on a single-shot 2D spin echo echo-planar imaging (ss-EPI) sequence. With this method, each slice is excited separately before the diffusion gradients are applied and the image information can be acquired with EPI encoding. As each single slice of the whole volume of interest has to be excited separately, this approach is inefficient with respect to the overall acquisition time (TA).[13] The overall TA can be

Editor: Michael Masoomi.

The authors report no conflicts of interest.

Institute of Diagnostic and Interventional Radiology, University Hospital Zürich, Zürich, Switzerland.

* Correspondence: Alexander Ciritsis, Institute of Diagnostic and Interventional Radiology, University Hospital Zürich, Rämistr. 100, 8091 Zürich, Switzerland (e-mail: alexander.ciritsis@usz.ch).

Medicine (2018) 97:32(e11745)

Received: 11 October 2017 / Accepted: 8 July 2018

http://dx.doi.org/10.1097/MD.0000000000011745

Table 1

Sequence parameters of the different T2w SPACE sequence and the DWI sequences with AF2, AF3, and AF3 performed with higher slice resolution.

	T2w-SPACE	Conventional DWI	SMS-DWI AF2	SMS-DWI AF3	SMS-DWI AF3 high res.
Multiband	No	No	Yes	Yes	Yes
Acceleration factor	–	–	2	3	3
Acquisition time, min:s	10.25	2:42	1:40	1:23	2:26
TR, ms	1500	5400	2800	1800	1800
TE, ms	96	52	57	60	60
Flip angle, °	150	90	90	90	90
Bandwith, Hz/Pixel	405	2330	2195	2195	2195
Number of slices	160	35	35	35	62
Slice thickness, mm	1	5	5	5	3
Voxel size, mm^3	$1.0 \times 1.0 \times 1.0$	$1.1 \times 1.3 \times 5$	$1.1 \times 1.3 \times 5$	$1.1 \times 1.3 \times 5$	$1.1 \times 1.3 \times 3$
Field of view, mm^2	339×380	307×381	307×381	307×381	307×381
GRAPPA acceleration factor	–	2	2	2	2

DWI = diffusion weighted sequences, GRAPPA = Generalized Autocalibrating Partial Parallel Acquisition, MRI = magnetic resonance imaging, SMS = simultaneous multislice, SPACE = sampling perfection with application optimized contrasts using different flip angle evolution, TE = echo time, TR = repetition time.

reduced using techniques of parallel imaging.[14,15] However, reduction of the acquisition time occurs at costs of image quality and of signal intensity.

The recently introduced simultaneous multislice (SMS) technique, which is often referred to as "multiband" excitation, offers a high potential to reduce scan time in DWI sequences.[16–19] In this acquisition scheme, instead of a consecutive excitation of slices, multiple slices are concurrently excited leading to a major decrease in scan time. The scan time reduction results from the shortening of the repetition time (TR), which is proportional to the applied acceleration factor and number of slices being excited. With the implementation of the blipped Controlled Aliasing in Parallel Imaging Results in Higher Acceleration (blipped CAIPIRIHIA) approach, SMS provides less restriction in signal-to-noise ratio (SNR) and overall image quality[20–22] compared with parallel imaging.

The purpose of this study was to evaluate the feasibility of SMS diffusion-weighted imaging (SMS-DWI) for lymph node assessment in the pelvic region. The SMS protocol was investigated regarding the number and depiction of lymph nodes detected with SMS DWI compared with conventional diffusion-weighted sequences, the most suitable SMS acceleration factor, the SNR, the contrast-to-noise ratio (CNR), and the overall TA. Furthermore, the benefit of SMS-DWI acquiring more slices with lower slice thickness in the same TA as in conventional diffusion-weighted sequences was assessed.

2. Material and methods

2.1. Study population

This prospective study was approved by the local ethics committee. After written informed consent was obtained, 8 healthy volunteers (4 men, 4 women; age range, 21–39 years; median age, 26 years) were included in this investigation.

2.2. Magnetic resonance imaging

MRI examinations were performed in supine position on a clinical 3T scanner, (MAGNETOM Skyra, Siemens Healthcare, Erlangen, Germany) using a flexible 18-channel body matrix coil and the built-in 32-channel spine coil for signal acquisition. The sequence protocols included 1 conventional single-shot EPI DWI protocol and 3 non-product SMS single-shot EPI DWI protocols with different acceleration factors (AF2 and AF3), and with AF3 but higher slice resolution, denoted "AF3 high res." Sequence parameters are listed in Table 1. Built-in post-processing software of the scanner was used to generate apparent diffusion coefficient (ADC) maps for each DWI sequence. Each DWI sequence was acquired twice with the exact same sequence parameters in order to calculate the SNR via the subtraction method.[23] Additionally, in order to establish a ground truth for the number of lymph nodes, an isotropic 3-dimensional T2-weighted fast-spin-echo sequence with high sampling efficiency (SPACE) for high spatial resolution[24] was acquired. The sequence parameters for the T2-weighted SPACE sequence were as follows: repetition time (TR): 1500 ms; echo time (TE): 96 ms; flip angle 180°; acquisition matrix $306 \times 380\,mm^2$; acquisition time: 10:25 minutes; number of signal averages: 2; pixel bandwidth 405 Hz/pixel (Table 1).

2.3. Image analysis

2.3.1. Lymph node detection. Two radiologists with >5 years of practical experience in pelvic MRI reviewed all acquired DWI sequences. In order to assess the ground truth for detected lymph nodes and for morphological correlation, both readers evaluated the isotropic high-resolution T2w 3D SPACE and determined the number of lymph nodes, which served as a reference standard (detection rate 100%). Furthermore, both readers assessed the number of detectable lymph nodes on the conventional DWI sequence as well as on the accelerated SMS-DWI on the $b = 800\,s/mm^2$ and $b = 0\,s/mm^2$ images.

2.4. Image quality

Datasets acquired with the b-value of $800\,s^2/mm$ were scored by both readers regarding image quality and overall artifacts using the following criteria: sharpness of lymph nodes, severity of artifacts, and overall image quality. Each criterion was classified according to a 5-score Likert scale, in which 5 points described best quality or most artifacts and 1 point described worst quality or fewest artifacts, respectively.

2.5. SNR

For each subject, circular regions of interest (ROI) (mean diameter: $0.40 \pm 0.06\,cm^2$) were placed into 4 representative lymph nodes on the conventional and all accelerated (AF2, AF3,

AF3 high-resolution) DWI sequences, respectively. In order to quantify noise, each of the twice performed DWI sequences with the highest b value ($b = 800\,s^2/mm$) were subtracted from each, and noise was defined as the standard deviation of the ROI signal in the subtracted sequences. SNR was then calculated as follows:

$$SNR = \sqrt{2} * \frac{SI_{lymphnode}}{Std.\,Dev._{noise}} \quad (1)$$

With $SI_{lymphnode}$ being the signal intensity in the ROI of the lymph node in the $b = 800\,s^2/mm$ DWI images and $Std.\,Dev._{noise}$ being the standard deviation of the signal intensity in the same ROI on the subtraction datasets. To minimize systematic errors due to motion, both sequences were registered to each other using dedicated software (syngo.via; Software Version VB10B, Siemens Healthcare, Erlangen, Germany).

2.6. SNR efficiency

For determination of the SNR efficiency, the ratio of SNR to acquisition time was calculated by dividing the previously determined average SNR by the corresponding square root of the TA of the sequence. The SNR efficiency of the accelerated DWI sequences was compared with the SNR efficiency of the conventional DWI, which served as a reference.

$$SNR_{efficiency} = \frac{SNR}{\sqrt{TA}} \quad (2)$$

2.7. Contrast-to-noise ratio

For contrast-to-noise ratio (CNR) calculation, a ROI analysis was performed for each volunteer on the acquired DWI $b = 800\,s^2/mm$ images. Circular ROIs (average diameter: $0.40 \pm 0.04\,cm^2$) were placed in the fatty tissue adjacent to the previously assessed ROIs in the lymph node, and CNR was calculated as follows:

$$CNR = \frac{SI_{fatty\ tissue} - SI_{lymph\ node}}{Std.\,Dev._{noise}} \quad (3)$$

with $SI_{fatty\ tissue}$ being the signal intensity in the ROI of the fatty tissue and $SI_{lymph\ node}$ and $Std.\,Dev._{noise}$ representing the previously determined signal intensity of the corresponding lymph node and standard deviation of noise, respectively.

2.8. ADC values

The built-in post-processing software of the MR scanner was used for calculation of ADC maps. To compare the reproducibility of ADC values for each DWI sequence, ADC values in lymph nodes were assessed in all performed DWI sequences using the same ROIs as in the SNR measurements.

2.9. Statistical analysis

Statistical analysis was performed using the SPSS software package (SPSS version 23, International Business Machines Corp., Armonk, NY). For all measured data (i.e., number of lymph nodes, SNR, CNR, and ADC), mean values and standard deviations were calculated. The inter-rater reliability of image quality scores was assessed, by calculating intra-class correlation (ICC) and evaluating them according to Landis and Koch.[25] To compare SNR, CNR, and ADC values between the individual DWI sequences, Wilcoxon test was used and P-values $<.05$ were considered as significant.

3. Results

3.1. Number of lymph nodes

All images were successfully acquired and ADC maps were generated for each DWI sequence in all cases (Figs. 1–3). All lymph nodes in the pelvis of each volunteer were successfully assessed by both readers, based on the highly resolved T2w 3D SPACE sequence (Fig. 2). The inter-rater agreement for lymph node detection in all acquired sequences (SPACE, conv. DWI, and SMS DWI) showed almost perfect agreement with ICC scores ranging between 0.959 and 0.996. Compared with the reference standard, the average detection rate of both readers for the conventional DWI was 89.6% and 69.4% (59.9%) for the SMS DWI sequences with AF2 (AF3), respectively. In the sequence with AF3 but higher slice resolution (AF3 high-resolution), an average detection rate of 83.0% was achieved (Fig. 4, Table 2).

3.2. Image quality

The rating for the overall image quality of the conventional DWI sequence ranged between 4 and 5 and was in average scored with

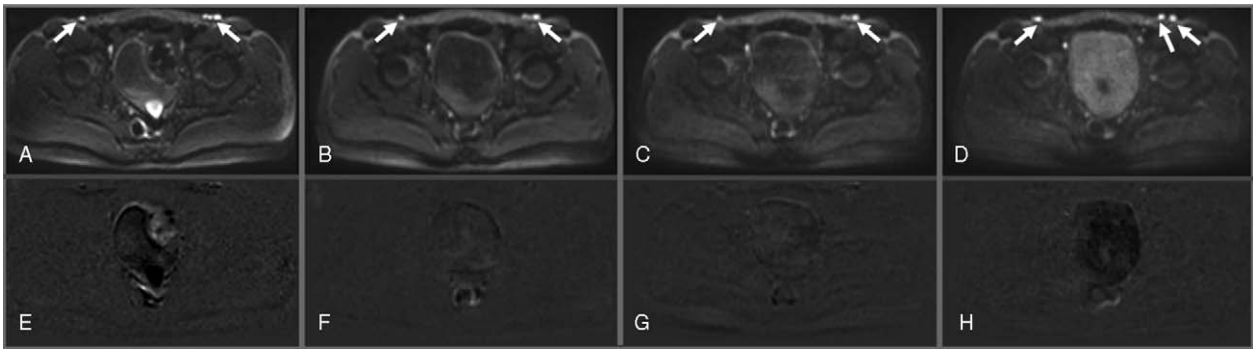

Figure 1. Examplary diffusion-weighted images with b-value of $800\,s/mm^2$. Two lymph nodes (arrows) in the abdominopelvic region are depicted. The upper row (A–D) shows different acceleration factors applied on the SMS-DWI. A: Conventional DWI; B: AF2; C: AF3; D: AF3 with higher slice resolution. The lower row (E–H) shows the corresponding subtraction dataset for the conventional (E) and each accelerated (F–H) DWI sequence used for measuring image noise and SNR calculation. DWI = diffusion weighted sequences, SMS = simultaneous multislice, SNR = signal to noise ratio.

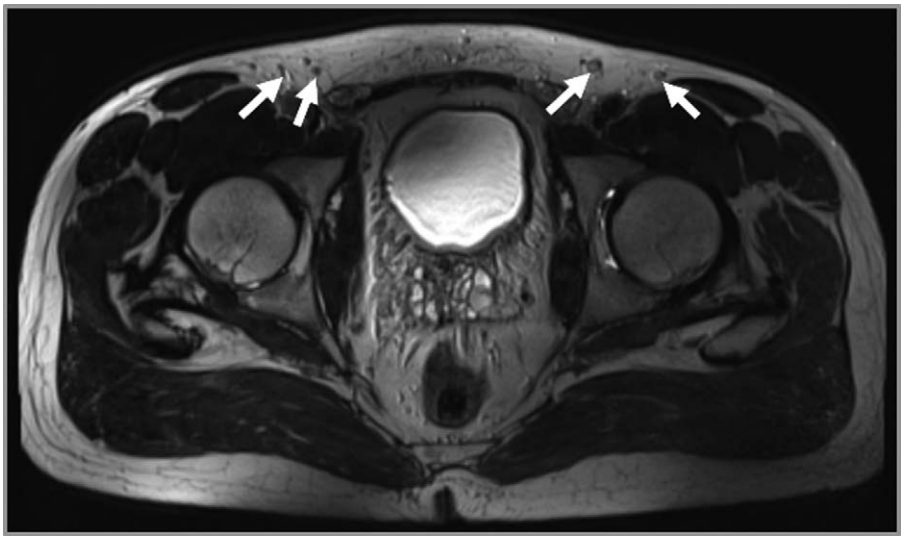

Figure 2. Image acquired with the T2-weighted high-resolution isotropic SPACE sequence. Four lymph nodes are shown (arrows). The number of lymph nodes detected on this sequence served as reference standard for the detection rate. SPACE = sampling perfection with application optimized contrasts using different flip angle evolution.

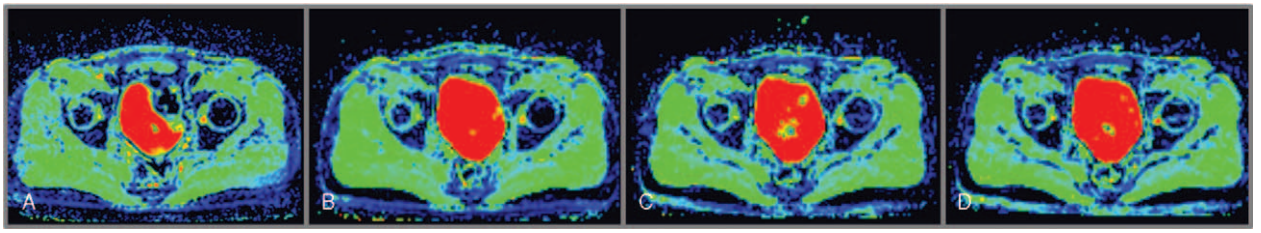

Figure 3. Exemplary ADC maps corresponding to the DWI images in Fig. 1A–D. ADC = apparent diffusion coefficient, DWI = diffusion weighted sequences.

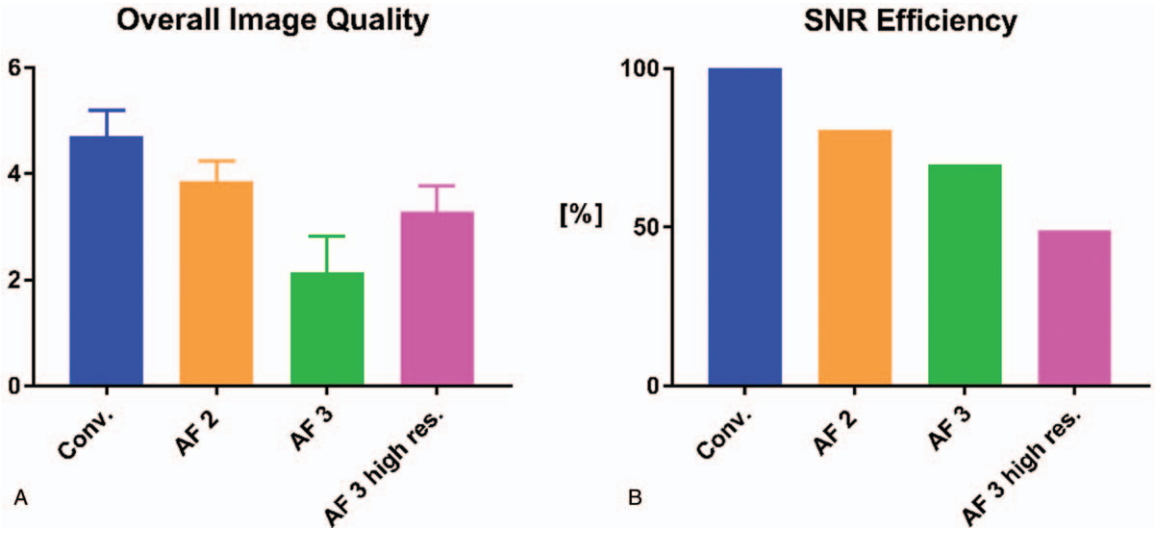

Figure 4. A: Average score on a 5-point Likert scale (1 = worst; 5 = best) for overall image quality evaluated by 2 radiologists for the conventional DWI sequence as well as each accelerated SMS-DWI sequence. B: Calculated SNR efficiency (SNR divided by the square root of the acquisition time of the corresponding sequence) for the all acquired DWI sequences. The conventional DWI sequence served as reference with an SNR efficiency of 100%. DWI = diffusion weighted sequences, SMS = simultaneous multislice, SNR = signal to noise ratio.

Table 2

Overview of the reader score evaluation for the different accelerated DWI sequences.

	SPACE	Conventional	AF2	AF3	AF3 high res.
Average number of lymph nodes	20.1 (20.3)	18.1 (18.1)	13.9 (14.1)	11.8 (12.4)	16.8 (16.7)
Detection rate, %	100 (100)	90.0 (89.2)	69.2 (69.5)	58.7 (61.1)	83.6 (82.3)
Severity of artifacts (1 = less/5 = most)	–	1.1 ± 0.35 (1.1 ± 0.35)	2.3 ± 0.45 (1.3 ± 0.45)	3.4 ± 0.90 (2.7 ± 0.70)	2.0 ± 0.53 (2.3 ± 0.14)
Sharpness/ Distinction of lymph nodes (1 = worst/5 = best)	–	4.4 (4.9)	3.3 (3.6)	1.9 (2.7)	3.6 (2.3)
Overall image quality	–	4.7 ± 0.45 (4.7 ± 0.45)	3.7 ± 0.45 (3.9 ± 0.35)	2.0 ± 0.53 (2.1 ± 0.63)	3.6 ± 0.49 (3.3 ± 0.45

DWI = diffusion weighted sequences, SPACE = sampling perfection with application optimized contrasts using different flip angle evolution.

4.7 (±0.01) by both readers. For the SMS-DWI sequences with AF2, AF3, and AF3 high-resolution, the overall image quality was rated by both readers on average with a score of 3.7 (±0.04), 2.1 (±0.04), and 3.4 (±0.07), respectively (Fig. 5A). The inter-rater agreement for overall image quality showed almost perfect agreement with an ICC value of 0.912. The scoring for the severity of artifacts amounted to 1.1 (±0.07) for the conventional DWI sequence, 1.8 (±0.5) for the DWI sequence with AF 2, and 3.1 (±0.35) and 2.1 (±0.14) for AF3 and AF3 with higher slice resolution. With respect to the inter-rater agreement, there was substantial agreement between the 2 raters reaching an ICC score of 0.714. Regarding the sharpness and distinction of the individual lymph nodes, there was almost perfect agreement between the 2 raters for all DWI sequences reaching an ICC value of 0.834. The average scoring of both readers for the conventional DWI sequence were 4.6 (±0.21), and 3.4 (±0.14), 2.7 (±0.42), and 3.4 (±0.64) for the DWI sequences with AF2, AF3, and AF3 high-resolution, respectively (Table 2).

3.3. SNR

For all accelerated sequences, the average SNR in the lymph nodes decreased with higher acceleration factor compared with conventional DWI ($P < .001$). The SNR of lymph nodes measured for the conventional DWI sequence was 46.1 (±20.6), whereas the SNR values of the SMS-DWI sequences with acceleration factors of 2 and 3 were 29.3 (±13.2) and 23.5 (±11.8). For the SMS-DWI with AF3 but higher slice resolution, the mean SNR was 21.5 (±9.4) (Fig. 4, Table 3).

3.4. $SNR_{efficiency}$

With increasing acceleration factor, the SNR efficiency decreased constantly and was significantly lower ($P < .001$) for SMS-DWI applying acceleration factors compared with conventional DWI. SNR efficiency decreased by 36.4%, 49.1%, and 52.6% for AF2, AF3, and AF3 high-resolution with respect to the conventional DWI sequence (Fig. 5B, Table 3).

3.5. CNR

The CNR decreased with increasing acceleration factor up to 46% for AF3 and was significant lower with $P < .001$ for all accelerated DWI sequences compared with the conventional DWI sequence (Fig. 4, Table 3).

3.6. ADC values

No significant differences were found between the ADC values in the evaluated lymph nodes of the accelerated DWI sequences as compared with the conventional DWI sequence (AF2: $P = .89$; AF3: $P = .69$; AF3 high-resolution: $P = .35$) (Fig. 3, Table 3).

4. Discussion

In the present study, we showed that the assessment of lymph nodes in the abdominopelvic region with accelerated SMS-DWI sequences is feasible. By applying an acceleration factor of 2 and thus reducing the acquisition time by approximately 40% it was still possible to detect 70% of the small healthy lymph nodes in the pelvic region compared with the highly resolved SPACE sequence. Compared with the DWI sequences, the high-resolution isotropic SPACE sequence was superior in terms of lymph node detection, as no relevant partial volume effects occurred and even the detection of very small lymph nodes was feasible. However, with an acquisition time of >10 minutes, the SPACE sequence is not compatible with the time restrictions of a clinical routine protocol for the detection of lymph nodes. An accelerated SMS DWI sequence with increased slice resolution, however, was able to almost reach the performance of the SPACE sequence with a detection rate of 83% (conventional DWI sequence 90%).

Implying only minimal losses in image quality compared with conventional DWI, an acceleration factor of 2 seems a good compromise between image quality, SNR, and acquisition time. As a conventional DWI sequence in the pelvic region exhibits an already fairly short acquisition time (2.42 minutes), the additional scan time gained through SMS acceleration, may also be used

Table 3

Quantitative values for SNR, CNR, ADC, and SNR efficiency of the DWI sequences with different acceleration factors.

	SPACE	Conventional	AF2	AF3	AF3 high res.
SNR	–	46.1 ± 20.6	29.25 ± 13.2	23.47 ± 11.8	21.46 ± 9.4
CNR	–	28.8 ± 15.5	21.8 ± 6.2	16.2 ± 8.1	15.6 ± 7.7
ADC ($\times 10^{-3}$ mm^2/s)	–	1.28 ± 0.26	1.27 ± 0.29	1.31 ± 0.28	1.24 ± 0.33
TA, min:s	–	2:42	1:40	1:23	2:26
SNR efficiency (SNR/$\sqrt{}$TA)	–	3.6	2.9	2.5	1.7

ADC = apparent diffusion coefficient, CNR = contrast to noise ratio, DWI = diffusion weighted sequences, SNR = signal to noise ratio.

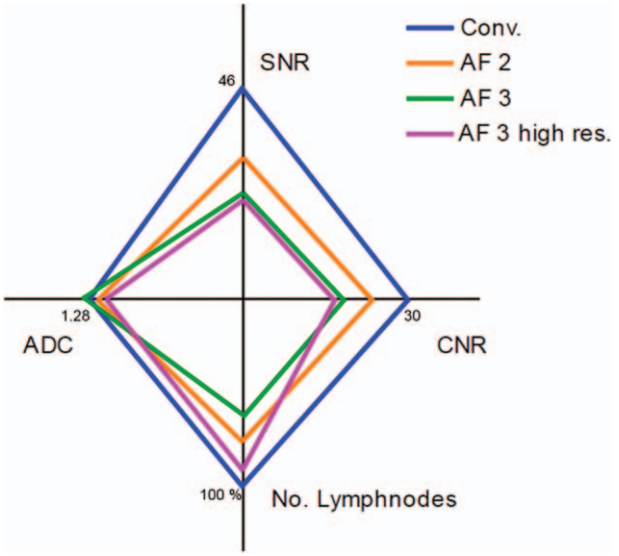

Figure 5. Web diagram qualitatively showing the performance of the conventional and accelerated SMS-DWI sequences regarding SNR, CNR, number of detected lymph nodes, and ADC value. The conventional DWI sequence performed best with respect to SNR and CNR; however, there was an almost equally high detection rate of lymph nodes for SMS-DWI with AF3 high-resolution. For all sequences, almost identical ADC values were observed. ADC = apparent diffusion coefficient, CNR = contrast to noise ratio, DWI = diffusion weighted sequences, SMS = simultaneous multislice, SNR = signal to noise ratio.

to increase slice resolution within the same acquisition time. This increase in spatial information and, thereby, reduction of partial volume effects may help to improve the detection of even small lymph node metastases, for example, in patients with prostate cancer, which is crucial for the selection of the appropriate treatment strategy.[12] By increasing the slice resolution by a factor of 2 as compared with conventional DWI, a detection rate of 83% was achieved, still offering a reduction of overall acquisition time by 10%. Furthermore, our results show that that there was no significant difference with respect to ADC accuracy when applying SMS-DWI with an acceleration factor of 2 or 3.

Nevertheless, the reduction of acquisition time also implies drawbacks when it comes to image quality. Particularly, for the SMS DWI sequence with an acceleration factor of 3 but equal spatial resolution as conventional DWI, the sharpness and distinction of lymph nodes, the severity of artifacts, and overall image quality was rated as inferior compared with conventional DWI or SMS AF2 sequences, especially resulting in difficulties to differentiate individual lymph nodes from each other.

This above described findings are in accordance with previous studies which evaluated the feasibility of SMS-DWI in different organs, for example, for the liver and pancreas imaging, as well as for the breast imaging, Boss et al and Filli et al, respectively.[22,26] In both previous studies, no significant deviations of ADC values were observed applying SMS-DWI with acceleration factors of 2 and 3 as compared with conventional DWI. Taking into account image quality, scan time reduction and ADC quantification accuracy, both studies concluded that an optimal acceleration factor of 2 poses the best compromise for clinical applicability.

Exhibiting only minor deviations for the ADC values, the additional acquisition time gained through SMS-DWI can be invested in the acquisition of a larger amount of *b*-values, especially in the low range. This might allow the implementation of an intravoxel incoherent motion (IVIM) model,[27] which in contrast to the conventional mono-exponential model for ADC calculation is based on a bi-exponential approach enabling a distinction of passive water diffusion (true diffusion) and the perfusion-related diffusion component (pseudo-diffusion) originating from capillary perfusion. In research, IVIM is increasingly used for tissue characterization such as liver fibrosis or treatment monitoring of malignant lesions. However, the additional acquisition of low *b*-values results in prolonged acquisition times of up to 15 minutes, which cannot be applied in a clinical protocol. However, SMS-DWI with its strong reduction of acquisition time may contribute to the implement IVIM into the clinical routine protocols with sufficient image quality for assessment of lymph nodes.

This study was performed on a cohort of healthy volunteers. Consecutively, we were not able to evaluate the detection rate, image quality, and ADC value accuracy of the applied SMS-DWI sequences in patients with malignant diseases. In fact, all sequences were acquired on volunteers without any diffusion restrictions or enlargement of the pelvic lymph nodes. However, patients are likely to exhibit diffusion restrictions as well as size increases of the abdominopelvic lymph nodes, especially for gynecological malignancies, prostate cancer, or rectal cancer. Therefore, the present study can be regarded as a worst-case scenario, whereas in clinical pathologies pathological lymph nodes will be easier to detect. Moreover, we believe that the inclusion of patients in this study would pose an additional limitation, as it would lead to a heterogeneous patient cohort due to the different diseases of each individual patient and no reliable ground truth would be available in order to determine the image quality and detection rate of SMS-DWI with different AFs. Therefore, the choice of SMS acceleration is even more warranted.

Nevertheless, it can be argued, that the relatively small number of study subjects included in this study posses an additional limitation. However, the results acquired with this relatively small study cohort are very homogenous and consistent, which is also supported by the almost perfect inter-rater agreement between both readers for image quality as well as for the detection rate for each SMS-DWI sequence. Due to these consistent results we believe that the acquired findings are reliable and would not significantly change by including a higher amount of study subjects.

Further study limitations need to be mentioned: In this study, the SNR values were determined via the subtraction method by measuring the standard deviation of the noise in the subtraction images of 2 identically acquired datasets. This method is one of various techniques in order to measure SNR and poses some limitation regarding registration errors due to motion. As an alternative, the acquisition of a second dataset for image subtraction could be avoided by measurement of the standard deviation of the noise in background air of the original image. However, this method does not account for sequences in which parallel imaging was applied due to the unequal distribution of parallel imaging induced noise in the image. In order to minimize the systematic errors due to motion, another approach to measure SNR is by acquiring an image consisting only of noise with radiofrequency transmission turned off.[28] The drawback of this approach is that only thermal noise in the receiver hardware is measured whereas noise in the transmission hardware is not captured. Moreover, in some MR scanners (also in ours) setting radiofrequency voltage to zero is not permitted. Taking into account these various pros and cons of the

different methods for SNR measurements, the subtraction technique represents one of the most feasible methods to calculate SNR. Dietrich et al[23] were able to show that it is reliable in in vivo measurements using parallel imaging. Furthermore, all images were acquired during free breathing without the application of a breathing belt or navigator. Although breathing induced triggering of the image acquisition may potentially result in better image quality compared with a free breathing protocol, a substantial prolongation of acquisition time would have been the consequence, which is generally not applicable in a clinical environment. Lastly, all images were acquired on a clinical 3.0T MR scanner, and different field strengths were not compared. However, similar findings may be expected at other field strengths as spin excitation and data readout for SMS-DWI is independent of the applied B0 field strength.

In conclusion, our study showed that, SMS-DWI is feasible for the detection and assessment of lymph nodes in the abdominopelvic region. Applying an acceleration factor of 2, a substantial reduction of acquisition time with only minor concessions regarding image quality was possible. In a setting with only healthy small lymph nodes and compared with a highly resolved SPACE sequence, averagely 90% of all lymph nodes in the pelvis were detected. The gained acquisition time via SMS may also be invested in a higher slice resolution instead of substantially reducing the overall scan time, leading to less partial volume effects and resulting in a detection rate of 83%. The best compromise between scan time reduction, image quality, and ADC accuracy was achieved applying an acceleration factor of 2.

Acknowledgments

The authors thank Markus Klarhöfer, PhD, Siemens Healthcare Switzerland, for his appreciated support.

Author contributions

Conceptualization: Alexander Ciritsis, Cristina Rossi, Andreas Boss.
Investigation: Alexander Ciritsis, Magda Marcon, Valerie Doan Phi Van.
Methodology: Alexander Ciritsis, Cristina Rossi.
Project administration: Andreas Boss.
Validation: Alexander Ciritsis.
Writing – original draft: Alexander Ciritsis.
Writing – review and editing: Alexander Ciritsis, Andreas Boss.

References

[1] Bihan D Le. Molecular diffusion nuclear magnetic resonance imaging. Magn Reson Q 1991;7:1–30.
[2] Bammer R. Basic principles of diffusion-weighted imaging. Eur J Radiol 2003;45:169–84.
[3] Donati OF, Chong D, Nanz D, et al. Diffusion-weighted MR imaging of upper abdominal organs: field strength and intervendor variability of apparent diffusion coefficients. Radiology 2014;270:454–63.
[4] Schmid-Tannwald C, Oto A, Reiser MF, et al. Diffusion-weighted MRI of the abdomen: current value in clinical routine. J Magn Reson Imaging 2013;37:35–47.
[5] Barabasch NA, Kraemer A, Ciritsis , et al. Diagnostic accuracy of diffusion-weighted magnetic resonance imaging versus positron emission tomography/computed tomography for early response assessment of liver metastases to Y90-radioembolization. Invest Radiol 2015;50: 409–15.
[6] Qayyum A. Diffusion-weighted imagining the abdomen and pelvis: concepts and applications. Radiographics 2009;29:1797–810.
[7] Koh DM, Collins DJ. Diffusion-weighted MRI in the body: applications and challenges in oncology. AJR Am J Roentgenol 2007;188:1622–35.
[8] Tang Y, Wang H, Wang Y, et al. Quantitative comparison of MR diffusion-weighted imaging for liver focal lesions between 3.0T and 1.5T: regions of interest of the minimum-spot ADC, the largest possible solid part, and the maximum diameter in lesions. J Magn Reson Imaging 2016;44:1320–9.
[9] Taouli B, Koh DM. Diffusion-weighted MR imaging of the liver. Radiology 2010;254:47–66.
[10] Chen YB, Liao J, Xie R, et al. Discrimination of metastatic from hyperplastic pelvic lymph nodes in patients with cervical cancer by diffusion-weighted magnetic resonance imaging. Abdom Imaging 2011; 36:102–9.
[11] Thoeny HC, Froehlich JM, Triantafyllou M, et al. Metastases in normal-sized pelvic lymph nodes: detection with diffusion-weighted MR imaging. Radiology 2014;273:125–35.
[12] Vallini V, Ortori S, Boraschi P, et al. Staging of pelvic lymph nodes in patients with prostate cancer: usefulness of multiple b value SE-EPI diffusion-weighted imaging on a 3.0 T MR system. Eur J Radiol Open 2016;3:16–21.
[13] Lewis S, Dyvorne H, Cui Y, et al. Diffusion-weighted imaging of the liver: techniques and applications. Magn Reson Imaging Clin N Am 2014;22:373–95.
[14] Pruessmann KP, Weiger M, Scheidegger MB, et al. SENSE: Sensitivity encoding for fast MRI. Magn Reson Med 1999;42:952–62.
[15] Griswold MA, Jakob PM, Heidemann RM, et al. Generalized autocalibrating partially parallel acquisitions (GRAPPA). Magn Reson Med 2002;47:1202–10.
[16] Feinberg DA, Setsompop K. Ultra-fast MRI of the human brain with simultaneous multi-slice imaging. J Magn Reson 2013;229: 90–100.
[17] Obele CC, Glielmi C, Ream J, et al. Simultaneous multislice accelerated free-breathing diffusion-weighted imaging of the liver at 3T. Abdom Imaging 2015;40:2323–30.
[18] Kenkel D, Barth BK, Piccirelli M, et al. Simultaneous multislice diffusion-weighted imaging of the kidney: a systematic analysis of image quality. Invest Radiol 2017;52:163–9.
[19] Fritz J, Fritz B, Zhang J, et al. Simultaneous multislice accelerated turbo spin echo magnetic resonance imaging: comparison and combination with in-plane parallel imaging acceleration for high-resolution magnetic resonance imaging of the knee. Invest Radiol 2017;52:529–37.
[20] Breuer FA, Blaimer M, Heidemann RM, et al. Controlled aliasing in parallel imaging results in higher acceleration (CAIPIRINHA) for multi-slice imaging. Magn Reson Med 2005;53:684–91.
[21] Setsompop K, Gagoski BA, Polimeni JR, et al. Blipped-controlled aliasing in parallel imaging for simultaneous multislice echo planar imaging with reduced g-factor penalty. Magn Reson Med 2012;67:1210–24.
[22] Filli L, Ghafoor S, Kenkel D, et al. Simultaneous multi-slice readout-segmented echo planar imaging for accelerated diffusion-weighted imaging of the breast. Eur J Radiol 2016;85:274–8.
[23] Dietrich O, Raya JG, Reeder SB, et al. Measurement of signal-to-noise ratios in MR images: influence of multichannel coils, parallel imaging, and reconstruction filters. J Magn Reson Imaging 2007;26:375–85.
[24] Lichy MP, Wietek BM, Mugler JP, et al. Magnetic resonance imaging of the body trunk using a single-slab, 3-dimensional, T2-weighted turbo-spin-echo sequence with high sampling efficiency (SPACE) for high spatial resolution imaging: initial clinical experiences. Invest Radiol 2005;40:754–60.
[25] Landis JR, Koch GG. The measurement of observer agreement for categorical data. Biometrics 1977;33:159–74.
[26] Boss A, Barth B, Filli L, et al. Simultaneous multi-slice echo planar diffusion weighted imaging of the liver and the pancreas: optimization of signal-to-noise ratio and acquisition time and application to intravoxel incoherent motion analysis. Eur J Radiol 2016;85:1948–55.
[27] Le Bihan D, Breton E, Lallemand D, et al. Separation of diffusion and perfusion in intravoxel incoherent motion MR imaging. Radiology 1988;168:497–505.
[28] Goerner FL, Clarke GD. Measuring signal-to-noise ratio in partially parallel imaging MRI. Med Phys 2011;38:5049–57.